Shahid Bahonar University of Kerman
Agricultural Biotechnology Journal
Iranian Biotechnology Society
Print ISSN: 2228-6705 Online ISSN: 2228-6500

Hepatoprotective of *Moringa oleifera* seeds extract loading chitosan nanoparticles (MOS-CNPs) via induction of gene expression of NRF2 against CCl_4-induced hepatic damage in male rats

Hayder Ali Sahib
Veterinary Medicine Collage, Al-Qasim Green University, 51013 Babylon, Iraq. E-mail: hayderali@vet.uoqasim.edu.iq

Hassan K. Al-Aawadi
Veterinary Medicine Collage, Al-Qasim Green University, 51013 Babylon, Iraq. E-mail: Dr.hassan@uoqasim.edu.iq

Hamzah H. K. Al-Shukri
* Corresponding author. Veterinary Medicine Collage, Al-Qasim Green University, 51013 Babylon, Iraq. E-mail: hamza.hashim@vet.uoqasim.edu.iq

Abstract

Objective

Liver diseases are a major health problem worldwide, and oxidative stress is involved in the pathogenesis of chemical-induced liver injury. *Moringa oleifera* (MO) seeds have potent antioxidant and hepatoprotective activities, which are, however, restricted by poor bioavailability. Chitosan nanoparticles (CNPs) are marketed as versatile delivery systems for bioactive compounds, offering improved pharmacokinetic profiles. The hepatoprotective and antioxidant potential of *Moringa oleifera* seeds ethanolic extract (MOSEE) loaded chitosan nanoparticles (CNPs) (MOS-CNPs) against carbon tetrachloride (CCl_4)-induced hepatic injury in male rats.

Materials and methods

Forty male rats were randomly divided into five groups (n=8): Control (normal saline/olive oil), CCl_4 only (negative control), CCl_4 and MOS extract, CCl_4 + MOS-CNPs Low dose and CCl4 + MOS-CNPs High dose. The experiment lasted 8 weeks. Biochemical markers of serum alanine aminotransferase (ALT), aspartate aminotransaminase (AST), alkaline phosphatase (ALP) total protein, and total bilirubin were measured. The antioxidant status was estimated by total antioxidant capacity (T-AOC) and malondialdehyde (MDA) levels. Liver tissue histopathology was analyzed and gene expression of NRF2 determined by qRT-PCR.

Results

CCl_4 treatment elevated serum ALT (217.95±9.87 U/L), AST (200.89±12.45 U/L), ALP (320.91±15.67 U/L) and TB (2.76±0.24 mg/dL) whilst decreased TP levels (4.15±0.28 g/dL)

when compared to control groups($p<0,001$). MOS-CNPs treatment dose-dependently reversed the above changes, and it had the best effect in high-dose group, such as ALT (77.96±5.12 U/L), AST (79.69±6.23 U/L), ALP (155.98±10.45 U/L), TB (0.99 ± 0.08 mg/dL) and TP (6.99 ± 0.32 g/dL). The activities of antioxidant markers in supplementation with MOS-CNPs 500 mg/kg markedly increased T-AOC (4.46±0.21 mmol/L) and lowered MDA (3.06±0.25 μmol/L) compared to the model group CCl_4 ($p<0.001$). The expression of the NFR2 gene was markedly increased by MOS-CNPs treated groups in contrast to CCl_4-intoxicated rats. Histopathological analysis confirmed the biochemical data showing decreased hepatocellular necrosis, inflammatory infiltration and fatty degenerescence.

Conclusion

MOS-CNPs have a better hepatoprotective and antioxidant effect as compared to free MOS extract by virtue of improved bioavailability and the controlled release pattern. The high-dose (500 mg/kg) provided the greatest protection against CCl_4-induced liver damage by regulating oxidative stress and activation of the NRF2 antioxidant signaling pathway.

Keywords: chitosan nanoparticles, hepatoprotection, liver enzymes, nanomedicine, oxidative stress

Paper Type: Research Paper.

Citation: Sahib, H. A., Al-Aawadi, H. K., & Al-Shukri, H. H. K. (2026). Hepatoprotective of *Moringa oleifera* seeds extract loading chitosan nanoparticles (MOS-CNPs) via induction of gene expression of NRF2 against CCl_4-induced hepatic damage in male rats. *Agricultural Biotechnology Journal,* 18(2), 467-488.

Agricultural Biotechnology Journal, 18(2), 467-488. DOI: 10.22103/jab.2026.26905.1862

Received: Decembre 24, 2025. Received in revised form: February 17, 2026.

Accepted: February 18, 2026. Published online: February 28, 2026.

Publisher: Shahid Bahonar University of Kerman & Iranian Biotechnology Society.

Introduction

Liver diseases are an enormous worldwide health burden with a death toll of around 2 million deaths per year globally (Asrani et al., 2019). The liver is the major metabolic and detoxification organ and it is very susceptible to damage by xenobiotics, drugs, alcohol, environmental pollutants. One of the best-characterized experimental models commonly used to study drug-induced liver injury and assess hepatoprotective agents is carbon tetrachloride (CCl_4)-induced hepatotoxicity (Sun et al., 2019; Algefare et al., 2024). The mechanism of CCl_4-induced liver injury is associated with the metabolic activation resulting from cytochrome P450 2E1 (CYP2E1) to produce trichloromethyl radical (CCl_3•), which further produces trichloromethyl peroxyl radical (CCl_3OO•) (Weiskirchen et al., 2019). These metabolites can promote lipid peroxidation cascades and membrane disruption in cells, as well upregulation of inflammatory cytokines

which ultimately lead to hepatocytes necrosis, fibrosis, cirrhosis (Hammad et al., 2023; Guo et al., 2025; Peng et al., 2025). Oxidative stress is the main mechanism of CCl_4 hepatotoxicity due to over production of reactive oxygen species (ROS) and decreasing level of endogenous antioxidants along with mitochondrial failure. A key regulator of cellular antioxidant defense is nuclear factor erythroid-related 2 (NRF2). Under basal conditions, NRF2 binds to KEAP1 and is then targeted for proteasomal degradation. During oxidative stress, NRF2 dissociates from KEAP1. It then translocates to the nucleus promoters (Cuadrado et al., 2019; Fuertes-Agudo et al., 2023). In the nucleus, it activates antioxidant response element (ARE)-dependent genes such as superoxide dismutase (SOD), catalase (CAT), glutathione peroxidase (GPx), glutathione S-transferases (GSTs), and NAD(P)H quinone oxidoreductase 1 (NQO1). When activated, the NRF2 pathway plays an important protective role against CCl_4-induced liver injury and fibrogenesis (Hammad et al., 2023; Guo et al., 2025; Peng et al., 2025). Snehal Pandurang Sonune moringa oleifera Lam., a member of family Moringaceae, is a fast-growing drought resistant tree species indigenous to Indian subcontinent and now distributed throughout the tropical countries and subtropical regions. Known as the “drumstick tree” or “miracle tree”, almost all parts of this plant including leaves, seeds, bark, roots, and flowers have medicinal and nutritional properties (Omeodu et al., 2022; Soto et al., 2025). *M. oleifera* seeds are rich in bioactive phytochemicals such as flavonoids (quercetin, kaempferol, myricetin), phenolic acids, glucosinolates (glucomoringin), isothiocyanates, alkaloids and terpenes (Singh et al., 2014; Abd-Elnaby et al., 2022; Pareek et al., 2023). These compounds demonstrate strong antioxidant, anti-inflammatory, antimicrobial and hepatoprotective properties. Particularly, the seed extract of *M. oleifera* has shown promising role in protecting against different hepatotoxic insults including paracetamol, alcohol and CCl_4-mediated liver injury (Pari and Kumar, 2002; Aly et al., 2020). *M. oleifera* has multiple pathways for the hepatoprotective mechanisms: direct free radical scavenging based on phenolic hydroxyl groups, increase of endogenous antioxidant enzyme activities, lipid peroxidation inhibition, modulation of inflammatory cytokine generation and hepatic cell membrane stabilization (Sun et al., 2019; Tao et al., 2022). Nevertheless, the therapeutic applications of traditional *M. oleifera* extracts often suffer from poor water solubility, low gastrointestinal absorption, rapid metabolism and short biological half-lives (Gao et al., 2025). Pharmaceutical research involving the development of targeted drug delivery systems, and with improved bioavailability, controlled release properties and minimized systemic toxicity has been transformed by nanotechnology. Chitosan, a cationic polysaccharide derived from chitin deacetylation, has been widely focused as a potential nanocarrier, due to its biocompatibility, biodegradability, mucoadhesive property and capability of crossing biological barriers (Rajabimashhadi et al., 2025; Jha and Mayanovic, 2023). On the other hand, nanotechnology is a multidisciplinary scientific field that uses a set of tools and techniques derived from engineering, physics, chemistry and biology (Mohammadabadi et al., 2009; Heidarpour et al. 2011; Mohammadabadi and Mozafari, 2018). Advances in nanoscience and nanotechnology have routinely enabled the fabrication and identification of submicron bioactive carriers. The delivery of bioactive substances to target sites in the body and their release behavior are directly affected by particle size (Mortazavi et al., 2005; Zarrabi et al., 2020). Compared to micrometer-sized

carriers, nanocarriers provide more surface area and have the potential to increase solubility, increase bioavailability, improve controlled release, and enable precise targeting of entrapped substances (Heidarpour et al. 2011; Mohammadabadi and Mozafari, 2019). Chitosan nanoparticle formulation Chitosan nanoparticles (CNPs) can be prepared under a variety of processing conditions such as ionic gelation, emulsion cross-linking, and polyelectrolyte complexation. The ionic gelation technique using TPP as a crosslinking agent is very favored because of its ease, mild preparation conditions and solvent free processing (Rajabimashhadi et al., 2025). A higher stability, sustained release and increased cellular uptake were proved for plant extracts loaded CNPs than the free extracts (Gao et al., 2025; Peng et al., 2025). Recent studies have revealed the therapeutic potential of CNPs in hepatic disorders. Chitosan-based nanocarriers have the ability to target liver due to their interaction with asialoglycoprotein receptors which are widely available on hepatocyte surfaces (Bonferoni et al., 2020). In addition, the positive charge of CNPs endows them with an ability to electrostatically interact with negatively charged cell membranes, thus enhancing cellular uptake and intracellular drug release (Guo et al., 2025; Peng et al., 2025). The present investigation aimed to develop Moringa oleifera seeds ethanolic extract loaded chitosan nanoparticles (MOS-CNPs) and assess the hepatoprotective and antioxidant efficacy of MOS-CNPs against CCl_4-induced hepatic damage in male rats. We anticipated that nanoencapsulation of MOS extract could improve its bioavailability and therapeutic activity in comparison with the free extract, through improving liver function markers, recovering antioxidant capacity, ameliorating the histopathological changes, and up-regulating expression of NRF2 gene.

Materials and methods

Chemicals and reagents: Carbon tetrachloride (CCl_4, MW 153.82 g/mol, purity 99.5%) was obtained from Sigmaâ, Aldrich (St. Louis, MO, USA). Chitosan (MW 300 KDa, deacetylation degree (DA)= 85%), sodium tripolyphosphate (TPP), and all other analytical grade chemicals were purchased from Merck (Darmstadt, Germany).

Preparation of *Moringa oleifera* seed ethanolic extract (MOSE): *Moringa oleifera* seeds were obtained from a certified botanical supplier and authenticated by a taxonomist at the Department of Botany. The seeds were cleaned, dried under shade, ground to fine powder mechanically in grinder. Maceration procedure was used for ethanolic extraction. In summary, the powdered seeds (500 g) were extracted with 2.5 L of 95% ethanol for 72 h at room temperature by gently shaking in-between. Whatman No.1 filter paper was used for filtering the extract, and the filtrate obtained was then concentrated under reduced pressure in a rotary evaporator at 40°C; followed by lyophilization and stored at -20°C until use. Yields of the extracts were determined and expressed as percentage (w/w).

Preparation of MOS-loaded chitosan nanoparticles (MOS-CNPs): Synthesis of MOS-CNPs MOS-CNPs were synthesized via ionic gelation method following the published modified protocols (Rajabimashhadi et al., 2025; Jha and Mayanovic, 2023). In short, chitosan (100 mg) was dissolved in a 1% aqueous solution of acetic acid (100 mL) under magnetic stirring. To the chitosan solution, MOS extract (using 50 mg in low dose and 100 mg in high dose) was

incorporated and stirred for 30 min. The TPP solution (0.5% w/v) was pipetted dropwise under continuous mixing (800 rpm) at room temperature until the opalescence signified NP formation. The nanoparticles were precipitated by using a centrifuged speed of 12,000 rpm for 30 min and rinsed with distilled water three times, followed by resuspension in phosphate-buffered saline (PBS: pH 7.4) to be in vivo used (Mohammed et al., 2025).

Characterization of MOS-CNPs: Average particle size, polydispersity index (PDI), and zeta potential were measured by dynamic light scattering (DLS) on a Zetasizer Nano ZS instrument (Malvern Instruments, UK). Morphological characterization was conducted by transmission electron microscope (TEM, JEM-1400, JEOL, Japan). EE and LC were determined after ultracentrifugation at 280 nm by UV – Vis Spectrophotometry. Invitro release studies of the formulations were performed in dialysis bags against PBS pH 7.4 at 37 °C with shaking 100 rpm. We used the following formulas to calculate the encapsulation efficiency (EE%) and loading capacity (LC%):

EE% = [(Total amount of MOS added − Free unencapsulated MOS) / Total amount of MOS added] × 100

LC% = [(Total amount of MOS added − Free unencapsulated MOS) / Total weight of nanoparticles] × 100

We used spectrophotometry at a wavelength of 280 nm to calculate the concentration of free MOS in the supernatant after ultrasound centrifugation.

Experimental animals and design: Adult male Wistar rats (8-10 weeks old weighing 180-220 g) were obtained from the animal house of the institute and kept under standard conditions in an environmentally controlled room (22±2°C, 12 h light/dark cycle, 55±5% humidity), with free access to standard pellet diet and water (Figure 1). Following acclimatization for 1 week, the rats were randomly assigned to five experimental groups (n=8 per group):

Control received an oral saline (2 mL/kg, orally) and an intraperitoneal (i.p.) injection of olive oil (1 mL/kg; i.p.) twice weekly for 8 weeks.

CCl_4 Group (negative control): Rats were treated with CCl_4 (1 mL/kg of 50% v/v in olive oil, i.p.) every twice a week for 8 weeks to induce hepatic fibrosis.

CCl_4+MOS 250 Group: Treated with CCl_4 as above and received MOS extract (250 mg/kg, p.o.) once daily for 8 weeks.

CCl_4 + MOS-CNPs 250 Group: Treated as above plus MOS-CNPs (250 mg/kg, p.o., equivalent to the dose of MOS extract) daily for 8 weeks.

CCl_4 + MOS-CNPs 500 Group: Rats were administered as above with CCl_4 plus daily MOS-CNPs (500 mg/kg, p.o.; equivalent of MOS extract) for 8 weeks.

The International Animal Care (IAC) and Use Com- mittee guidelines were adhered to, and the animal experimental protocol was approved by the Al-Qasim green University Animal Ethics Committee (AGUAEC Approval No. /2025/112).

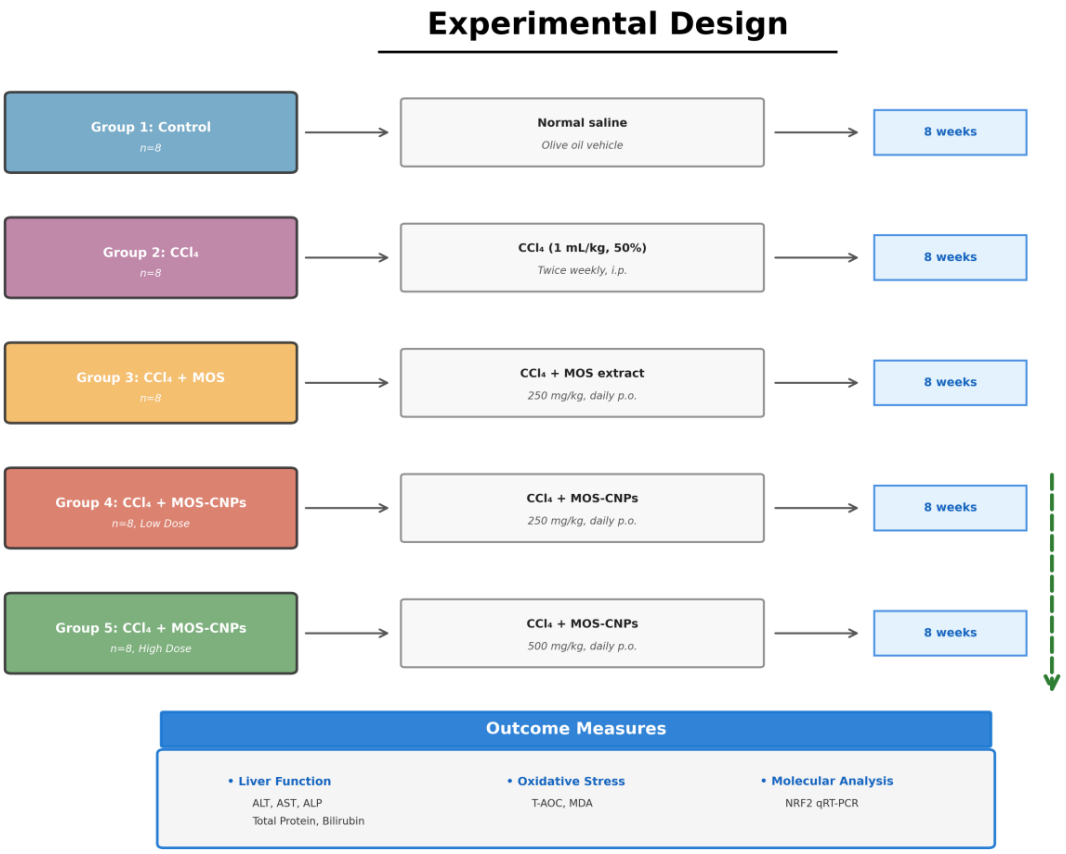

Figure 1. Flowchart illustrating the experimental protocol. Shows five treatment groups with sample sizes, treatment regimens, 8-week duration, and outcome measures

Specimen collection and biochemical measurements: The animals were fasted during one night and anaesthetized with ketamin-xylazine (80:10 mg/kg, i.p.) at the end of an 8-week experimental period. Blood samples were collected by cardiac puncture, clotted for 30 minutes and centrifuged at 3,000 rpm for 15 minutes to produce serum. Liver tissues were immediately excised, washed in ice-cold saline and divided into three parts; the first part was fixed in 10% neutral buffered formalin for histopathology examination, the second part was frozen in liquid nitrogen for gene expression analysis, and the third was homogenized for oxidative stress markers. Serum liver function indexes were detected by using commercial diagnostic kits on an automated biochemistry analyzer (Mindray BS-2800M, China): alanine aminotransferase (ALT, UV-kinetic method), aspartate aminotransferase (AST, UV-kinetic method), alkaline phosphatase (ALP, p-nitrophenyl phosphate method), total protein (TP, biuret method) and total bilirubin (TB, diazo method).

Determination the levels of oxidative stress markers: Tissue Homogenates Liver homogenates (10% w/v) were prepared in ice-chilled PBS by Teflon glass with tissue grinder. T-AOC was determined by the ferric reducing antioxidant power (FRAP) assay of Benzie and Strain (1996) as mmol Fe^{2+} /L. The formation of thiobarbituric acid reactive substances (TBARS), as

an indicator of lipid peroxidation, was measured according to Esterbauer and Cheeseman (1990) and expressed in g/g tissue.

Quantitative real-time PCR (qRT-PCR) for assessment of NRF2 gene expression: Liver frozen tissue was used for total RNA extraction with TRIzol reagent (Invitrogen, USA) according to the manufacturer's instruction. The purity and concentration of RNA was checked by a NanoDrop spectrophotometer (Thermo Fisher Scientific, USA). cDNA was prepared from 2 µg total RNA with the High-Capacity cDNA Reverse Transcription Kit (Applied Biosystems, USA). Real-time quantitative PCR (qRT-PCR) was conducted with SYBR Green Master Mix reagent (Roche, Germany) on a QuantStudio 5 Real-Time PCR system (Applied Biosystems, USA). Q-PCR primers used were for rat NRF2 (forward primer: 5'-AGCAGCAGCAGCATGACTGA-3', reverse primer: 5'-GTGGGCAACCTGGGAGTAGAT-3') and the housekeeping gene β actin (forward primer: 5'-CCCATCTATGAGGGTTACGC-3', reverse primer: 5'-TTTAATGTCACGCACGATTTC-3'). The cycling conditions were as follows: 95°C for 10 minutes and then 40 cycles of 95°C for 15 seconds, 60°C for one minute. The $2^{-\Delta\Delta Ct}$ method was used to determine the relative gene expression (Livak and Schmittgen, 2001).

Histopathological examination: For the histopathological analysis, liver tissues were collected, weighed, and representative sections (approximately 0.5 cm in thickness) fixed in 10% neutral-buffered formalin for 24 hours. The resulting tissues were further processed with graded series of ethanol and xylene, paraffin embedded, cut at 4–5 µm on a rotary microtome and histologically stained with hematoxylin-eosin (H&E). Sections from all lobes were reviewed and scored by a licensed veterinary pathologist blinded to the treatment groups, using a semi-quantitative scoring system that evaluated the organization of hepatocytes and portal areas, sinusoidal dilation, necrosis, vascular congestion, and inflammatory infiltrate.

Statistical analysis

Results are expressed as mean ± SD. Statistical analysis was carried out by one-way ANOVA followed by Tukey post-hoc test for multiple comparisons, using GraphPad Prism version 9.0 (GraphPad Software, USA). Differences were taken as significant at p 0.05 vs. Control).

Results and discussion

Characterization of MOS-CNPs: Formation of the MOS-loaded chitosan nanoparticles was successfully carried out by ionic gelation technique. Characterization The average particle size of the MOS-CNPs was 187.34 ± 12.56 nm and had a polydispersity index (PDI) of 0.24 ± 0.03, meaning that it had an uniform narrow size distribution after particle-size characterization studies were conducted on them and proved as shown in Figure 2. The zeta potential was +32.45 ± 2.18 mV, implying a positive surface charge that enhances stability and cellular uptake efficiency. SEM and TEM image showed the round shape of nanoparticles, smooth surface and good distribution (Figure 2A, B). The encapsulation efficiency (EE%) of MOS extract in chitosan nanoparticles was 84.6 ± 3.2%. This result indicates that the loading of bioactive compounds was successful. The loading capacity (LC%) was 18.4 ± 1.6%. This capacity indicates the effective incorporation of MOS into the nanoparticle matrix. In vitro release results revealed a biphasic

release profile comprising an initial burst release (about 35% within first 4 h) followed by sustained-release for 48 h (>78.5 ± 4.3%, Table 1, Figure 2C). This profile of release is desirable to assure that therapeutic levels are not exceeded for too long intervals. The FT-IR spectrum illustrates the Moringa oleifera seeds ethanolic extract loaded chitosan nanoparticles (MOS-CNPs) with characteristic absorbance bands related to both the chitosan polymer matrix and bioactive compounds encapsulated from M. *oleifera* seeds. FTIR data spectrum was obtained in the region of 4000-400 cm^{-1} with a Shimadzu FT-IR spectrophotometer (Figure 2D).

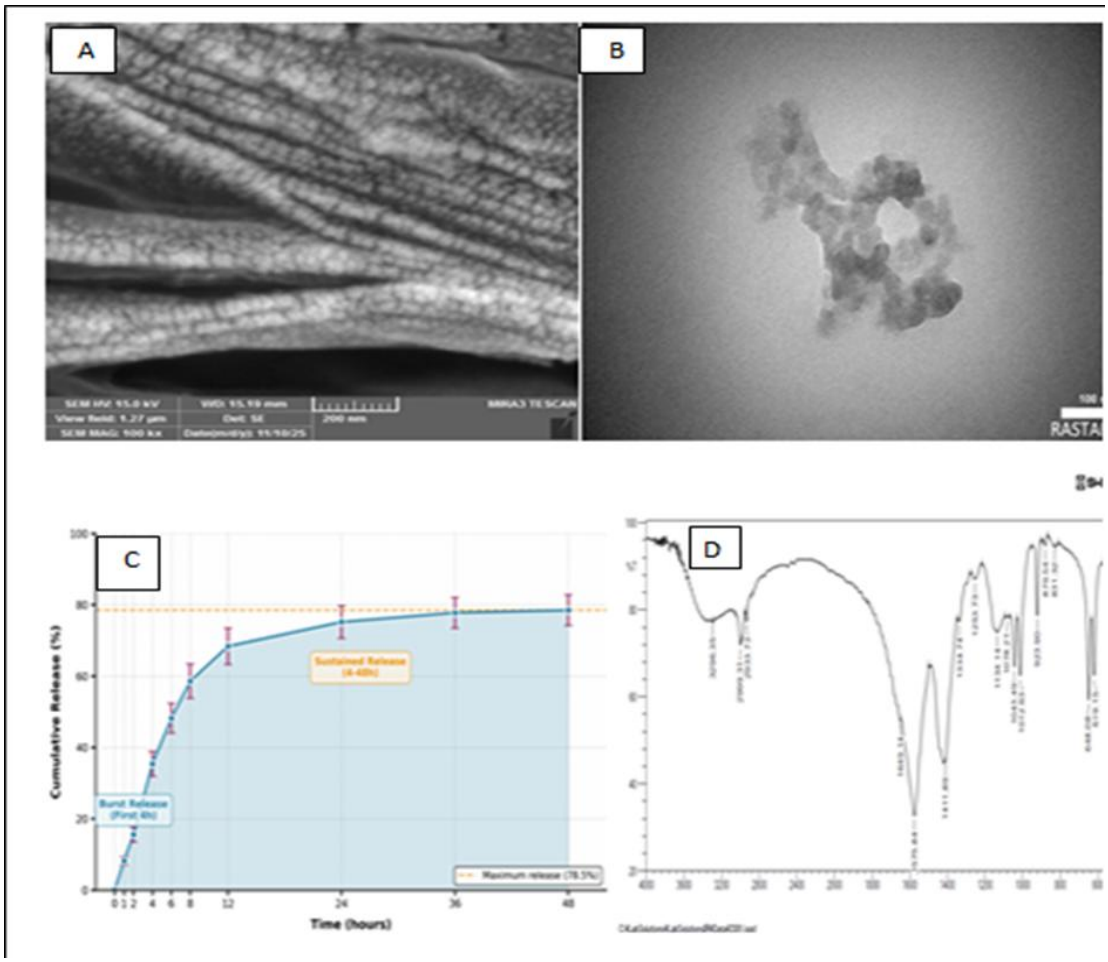

Figure 2. Characterization of *Moringa oleifera* seeds extract-loaded chitosan nanoparticles (MOS-CNPs). (A) scanning electron microscopy (SEM) image showing average particle size of 187.34 ± 12.56 nm. (B) Transmission electron microscopy (TEM) image showing spherical morphology with uniform distribution. (C) In vitro release % of MOS-CNPs. (D) FT-IR analysis of MOS-CNPs

The FT-IR spectrum of MOS-CNPs in Figure 2D, shows that the wide, strong absorption band occurred at wavenumber of 3296.35 cm^{-1} is overlapped O-H and N-H stretching vibrations arising from the hydroxyl groups such as chitosan, primary amino group and phenolic hydroxide belong extracted compound loading. The significant broadness of this peak (wavenumber region bearing around 3600–3300 cm^{-1}) reflects intense intermolecular as well as intramolecular

hydrogen bonds in the nanoparticle matrix which certainly contributes to structural stability and sustained release behaviour of MOS-CNPs. The band was shifted toward lower wavenumber from the free hydroxyl stretching, indicating strong hydrogen bonding interaction between chitosan and bioactive compounds. The aliphatic C-H stretching bands are observed at 2999.31 and 2933.73 cm^{-1} assigned to asymmetric and symmetric stretching, respectively, of the methylene/methyl moieties common to both the chitosan polysaccharide backbone as well as lipids, alkaloids and terpenoids found in *M. oleifera* seed extract). The amide region of 1700 and 1500 cm-1 plays a vital role in the identification of chitosan and its degree of acetylation. The maximum at 1649.14 cm^{-1} could be attributed to the amide I band (C=O stretching) of residual N-acetylglucosamine units in chitosan; however, it overlapped with C=C stretching vibrations deriving from the flavonoids and phenolic compounds contained by extract. The strong peak at 1575.84cm^{-1} corresponds to Amide II (N-H bending coupled with C-N stretching) which is assigned for primary amino group of chitosan. The appearance of both Amide I and Amide II bands is an indication that the chitosan polymer used," CER" in this work, was incompletely acetylated with 75-85% extent of deacetylation (Dd), similar to our starting material for nanoparticles. Those amide bands also showed that the chitosan preserved its structural integrity following ionotropic gelation with sodium tripolyphosphate.

Effects on liver function markers-Serum ALT, AST, and ALP): Treatment with CCl_4 caused severe hepatocellular damage as indicated by pronounced increase in both serum ALT and AST activities compared to control group (p0.001 vs.CCl_4, $p<0.05$ vs Control). The CCl_4 group exhibited ALT levels of 217.95±9.87 U/L (approximately 5-fold increase) and AST levels of 200.89±12.45 U/L (approximately 3.8-fold increase) relative to control values (Table 1). Treatment with MOS extract (250 mg/kg) partially attenuated these elevations, reducing ALT to 142.85±10.23 U/L and AST to 125.91±9.87 U/L ($p<0.001$ vs. CCl_4 group). Notably, MOS-CNPs demonstrated superior hepatoprotective effects in a dose-dependent manner. The MOS-CNPs 250 mg/kg group showed further reductions in ALT (92.65±8.34 U/L) and AST (95.19±7.45 U/L) compared to the free extract group ($p<0.01$). The high dose MOS-CNPs (500 mg/kg) achieved the most significant protection, normalizing ALT (77.96±5.12 U/L) and AST (79.69±6.23 U/L) to levels approaching the control group ($p<0.001$ vs. CCl_4, $p>0.05$ vs. Control). ALP activity was significantly elevated in the CCl_4 group (320.91±15.67 U/L) compared to controls (98.19±6.78 U/L), indicating cholestatic injury and biliary dysfunction ($p<0.001$). MOS extract treatment reduced ALP to 208.85±12.34 U/L ($p<0.001$ vs. CCl_4). MOS-CNPs 250 and 500 mg/kg further decreased ALP levels to 169.48±9.87 U/L and 155.98±10.45 U/L, respectively ($p<0.001$ vs. CCl_4, $p<0.01$ vs. MOS extract). The high dose MOS-CNPs restored ALP to within normal physiological range (Figure 3).

Serum total protein and total bilirubin: CCl_4 intoxication significantly decreased serum total protein (4.15±0.28 g/dL) and increased total bilirubin (2.76±0.24 mg/dL) compared to control values (7.18±0.34 g/dL and 0.48±0.06 mg/dL, respectively; $p<0.001$), reflecting impaired hepatic synthetic function and excretory capacity. All treatment groups showed dose-dependent improvements in these parameters. The MOS-CNPs 500 mg/kg group demonstrated the most

pronounced restoration of total protein (6.99±0.32 g/dL) and bilirubin (0.99±0.08 mg/dL), with the protein levels being statistically comparable to controls ($p>0.05$) (Figure 4).

Table 1. Effects of MOS-CNPs on serum liver function markers in CCl_4-induced hepatotoxicity

Group	ALT (U/L)	AST (U/L)	ALP (U/L)	Total Protein (g/dL)	Total Bilirubin (mg/dL)
Control	43.75±5.12	52.83±5.67	98.19±6.78	7.18±0.34	0.48±0.06
CCl_4	217.95±9.87***	200.89±12.45***	320.91±15.67***	4.15±0.28***	2.76±0.24***
CCl_4 + MOS 250	142.85±10.23***†††	125.91±9.87***†††	208.85±12.34***†††	5.27±0.31***††	1.75±0.18***††
CCl_4 + MOS-CNPs 250	92.65±8.34***†††‡‡	95.19±7.45***†††‡‡	169.48±9.87***†††‡‡	6.24±0.29***†††‡‡	1.34±0.12***†††‡‡
CCl_4 + MOS-CNPs 500	77.96±5.12***†††‡‡§§	79.69±6.23***†††‡‡§§	155.98±10.45***†††‡‡§§	6.99±0.32***†††‡‡§§	0.99±0.08***†††‡‡§§

*Data are expressed as mean ± SD (n=8). ***p<0.001 vs. Control; †††p<0.001 vs. CCl_4; ‡‡p<0.01 vs. CCl_4+MOS 250; §§p<0.01 vs. CCl_4+MOS-CNPs 250.*

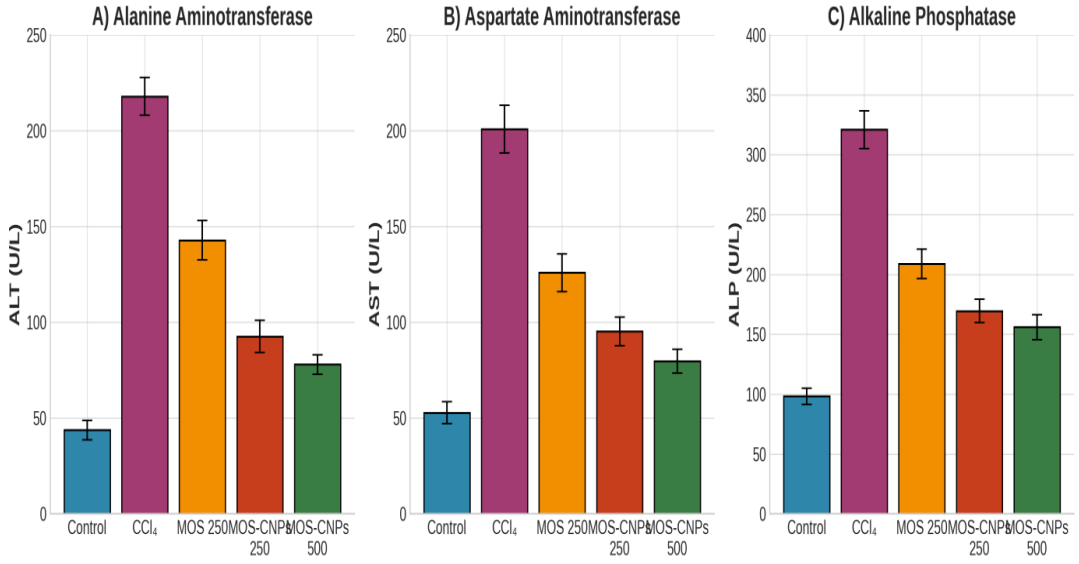

Figure 3. Effects of MOS-CNPs on serum liver enzymes in CCl_4-induced hepatotoxicity. (A) ALT, (B) AST, and (C) ALP levels were significantly elevated in the CCl_4 group and dose-dependently reduced by MOS-CNPs treatment. Values are mean ± SD (n=8). ***p<0.001 vs. Control; †††p<0.001 vs. CCl_4; ‡‡p<0.01 vs. CCl_4+MOS 250; §§p<0.01 vs. CCl_4+MOS-CNPs 250

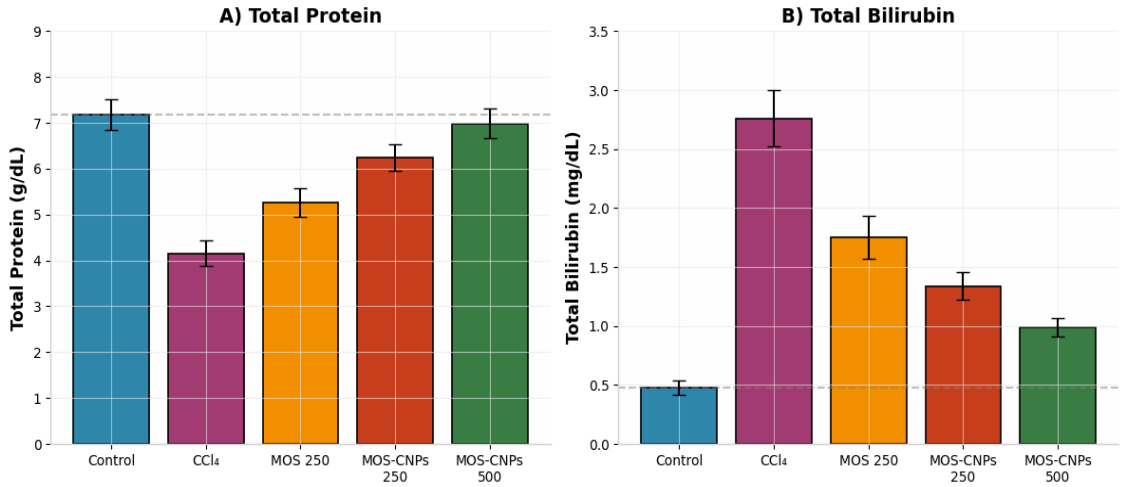

Figure 4. Effects of MOS-CNPs on hepatic synthetic and excretory function. (A) Total Protein and (B) Total Bilirubin levels showing impaired function in CCl_4 group and restoration by MOS-CNPs. Dashed lines indicate control levels. Values are mean ± SD (n=8)

Effects on oxidative stress markers-Total antioxidant capacity (T-AOC): Hepatic T-AOC was significantly depleted in the CCl_4 group (1.35±0.11 mmol/L) compared to controls (5.41±0.23 mmol/L), indicating severe oxidative stress and consumption of endogenous antioxidants ($p<0.001$; Table 2). Treatment with MOS extract at 250 mg/kg partially restored T-AOC to 3.03±0.18 mmol/L ($p<0.001$ vs. CCl_4). MOS-CNPs demonstrated superior antioxidant enhancement, with the 250 mg/kg dose increasing T-AOC to 3.74±0.21 mmol/L and the 500 mg/kg dose achieving 4.46±0.21 mmol/L ($p<0.001$ vs. CCl_4, $p<0.01$ vs. MOS extract). The high dose MOS-CNPs restored approximately 82% of the total antioxidant capacity compared to controls.

Table 2. Effects of MOS-CNPs on hepatic oxidative stress markers

Group	T-AOC (mmol/L)	MDA (µmol/g tissue)
Control	5.41±0.23	2.32±0.15
CCl_4	1.35±0.11***	8.76±0.34***
CCl_4 + MOS 250	3.03±0.18***†††	5.55±0.28***†††
CCl_4 + MOS-CNPs 250	3.74±0.21***†††‡‡	4.38±0.22***†††‡‡
CCl_4 + MOS-CNPs 500	4.46±0.21***†††‡‡§§	3.06±0.25***†††‡‡§§

*Data are expressed as mean ± SD (n=8). ***p<0.001 vs. Control; †††p<0.001 vs. CCl_4; ‡‡p<0.01 vs. CCl_4+MOS 250; §§p<0.01 vs. CCl_4+MOS-CNPs 250*

Malondialdehyde (MDA) levels: Lipid peroxidation, quantified by MDA levels, was dramatically elevated in the CCl_4 group (8.76±0.34 µmol/g tissue) compared to controls (2.32±0.15 µmol/g tissue; $p<0.001$), confirming extensive membrane damage (Esterbauer & Cheeseman, 1990). MOS extract treatment significantly reduced MDA to 5.55±0.28 µmol/g tissue ($p<0.001$ vs. CCl_4). MOS-CNPs exhibited more potent anti-lipid peroxidation effects, with MDA levels of 4.38±0.22 µmol/g tissue at 250 mg/kg and 3.06±0.25 µmol/g tissue at 500 mg/kg ($p<0.001$ vs. CCl_4, $p<0.01$ vs. MOS extract). The high dose MOS-CNPs reduced MDA by 65%

compared to the CCl_4 group and by 45% compared to the free extract group. Figure 5 showing (A) Total Antioxidant Capacity (T-AOC) and (B) Malondialdehyde (MDA) levels. T-AOC is significantly depleted in CCl_4-treated rats, while MDA (lipid peroxidation marker) is elevated. MOS-CNPs treatment reverses these changes in a dose-dependent manner.

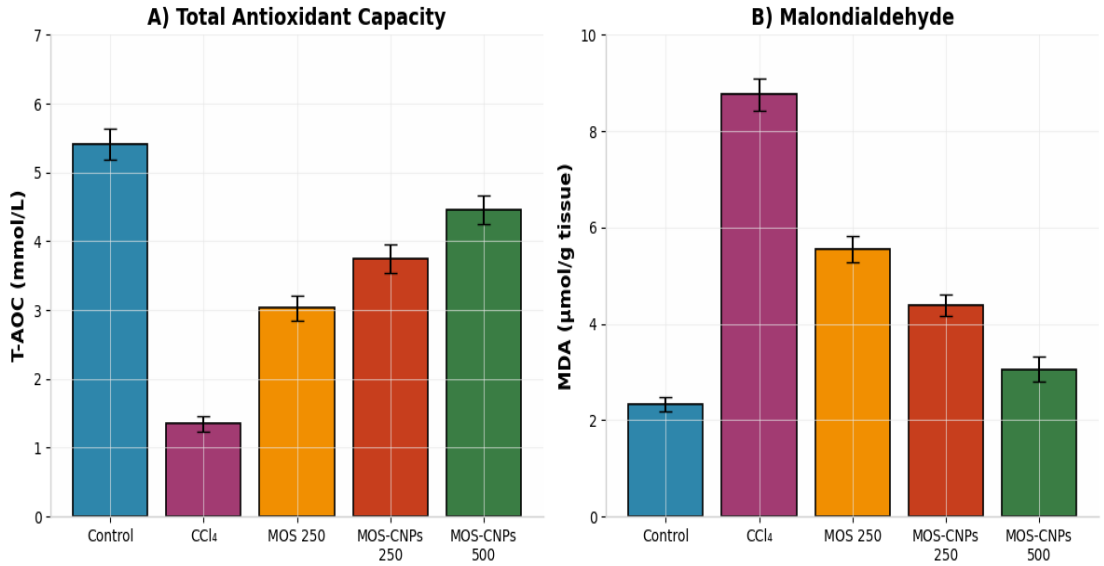

Figure 5. Effects of MOS-CNPs on oxidative stress markers. (A) Total Antioxidant Capacity (T-AOC) and (B) Malondialdehyde (MDA) levels demonstrating antioxidant efficacy. Values are mean ± SD (n=8)

NRF2 gene expression analysis: Quantitative RT-PCR analysis revealed significant downregulation of NRF2 gene expression in the CCl_4 group (0.42±0.08 fold change relative to control; $p<0.001$), consistent with impairment of the antioxidant defense system under chronic oxidative stress. Treatment with MOS extract upregulated NRF2 expression to 1.85±0.15 fold ($p<0.001$ vs. CCl_4). MOS-CNPs demonstrated superior activation of the NRF2 pathway, with the 250 mg/kg dose increasing expression to 2.34±0.18 fold and the 500 mg/kg dose achieving 3.12±0.21 fold compared to control ($p<0.001$ vs. CCl_4, $p<0.01$ vs. MOS extract). These findings indicate that nanoencapsulation significantly enhances the ability of *M. oleifera* extract to activate the master antioxidant regulator NRF2 (Cuadrado et al., 2019; Fuertes-Agudo et al., 2023). Figure 6 showing NRF2 gene expression (fold change relative to control) measured by qRT-PCR. CCl_4 downregulates NRF2, while MOS-CNPs cause significant upregulation, with the high dose showing 3.12-fold increase over control.

Histopathological findings: The individual biochemical data was well mirrored in the histopathological examinations of H&E-stained liver sections (Figure 7 and Table 3). Liver sections from the control group (panels A and B) revealed normal hepatic architecture with well-structured cords of hepatocytes radiating around the central vein, widely patent sinusoids with narrow lumina, and organized portal areas without inflammatory cell infiltrates or necrosis. The liver cells had large nuclei and finely granular eosinophilic cytoplasm with distinctly defined cell

borders. In the positive control group of CCl4 (panels C and D), extensive necrosis of hepatocytes, vascular congestion accompanied by notable dilatation of central veins and hepatic vessels, widened sinusoids with remarkable congestion and dense aggregation of inflammatory cells around portal area characterized severe hepatic damage.

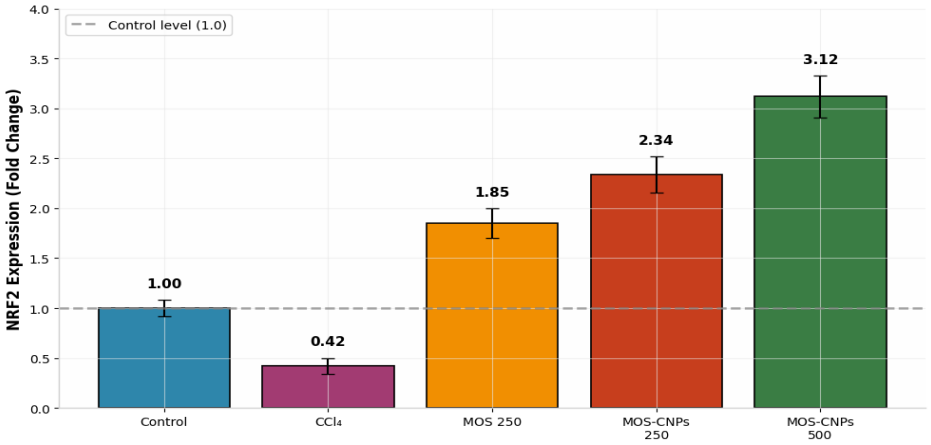

Figure 6. NRF2 gene expression in liver tissue measured by qRT-PCR. MOS-CNPs significantly upregulated NRF2 expression in a dose-dependent manner. Values are fold change relative to control (mean ± SD, n=8)

The lobular architecture appeared profoundly disrupted, there was patchy microstrome congestion, and large areas of the hepatic parenchyma were characterized by loss of nuclear integrity consistent with centrilobular necrosis. In Group 3 (CCl4 + crude MOSE, 250 mg/kg; panel E), the partial hepatoprotection was observed. Although vascular congestion was profoundly diminished in most stromal areas, there were residual heterogenously scattered necrotic foci along with hepatocytic hyperplasia. Inflammatory cell aggregation persisted in the liver indicating sustained but blunted inflammatory responses. Group 4 (CCl4 + MOSE-CNPs, 250 mg/kg) exhibited a significantly ameliorated hepatic architecture– well-lobulated stroma, orderly arrangement of hot hepatocytes losing degenerative foci and well-organized portal areas as shown in panel F. There remained inflammatory cell infiltration in some liver lobules, indicating the liver continued to be in a phase of active repair and resolution. Group 5 (CCl4 + MOSE-CNPs, 500 mg/kg) exhibited the best histological recovery (panel G), with H&E staining similar to that of the control group, where the structure and arrangement of hepatocytes were intact; no vacuolation was seen in the liver sections; cell borders were distinguished clearly in a lobular pattern; cytoplasm was strongly eosinophilic and granular. Portal areas were well-defined and there was no necrosis at all, and only subtle residual inflammatory infiltration. Figure 8 shows the Schematic diagram proposing the mechanism of hepatoprotection by MOS-CNPs. Shows progression from CCl_4 injury through MOS-CNPs intervention to final hepatoprotection, with detailed molecular mechanisms including antioxidant, anti-inflammatory, anti-fibrotic, and membrane stabilization pathways. The present study offers convincing proof that Moringa oleifera seed ethanolic extract-loaded chitosan nanoparticles (MOS-CNPs) are much stronger hepatoprotective and antioxidant than free MOS extract into rats with CCl_4-induced hepatic

damage. Advantages of MOS-CNPs are higher bioavailability, prolonged release profile and directed hepatic delivery mediated via chitosan nanocarrier system (Gao et al., 2025).

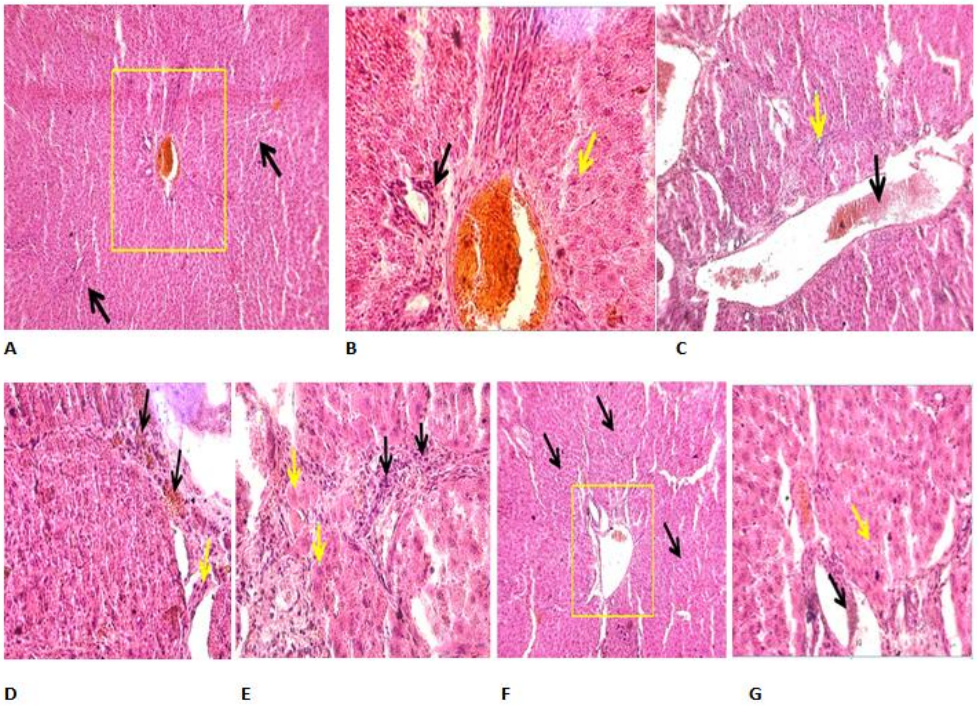

Figure 7. Representative H&E-stained liver sections showing histopathological changes in different experimental groups (magnification ×200)

Table 3. Histopathological scoring of liver tissue alterations

Group	Necrosis	Fatty Degeneration	Inflammation	Congestion	Overall Score
Control	0 ± 0^{a}	0 ± 0^{a}	0 ± 0^{a}	0 ± 0^{a}	0 ± 0^{a}
CCl_4	3.0 ± 0.0^{b}	3.0 ± 0.0^{b}	3.0 ± 0.0^{b}	3.0 ± 0.0^{b}	3.0 ± 0.0^{b}
CCl_4 + MOS 250	1.8 ± 0.4^{c}	1.5 ± 0.5^{c}	1.5 ± 0.5^{c}	1.3 ± 0.5^{c}	1.5 ± 0.3^{c}
CCl_4 + MOS-CNPs 250	1.0 ± 0.4^{d}	0.8 ± 0.4^{d}	0.8 ± 0.4^{d}	0.5 ± 0.5^{d}	0.8 ± 0.3^{d}
CCl_4 + MOS-CNPs 500	0.3 ± 0.3^{e}	0.3 ± 0.3^{e}	0.3 ± 0.3^{e}	0.3 ± 0.3^{e}	0.3 ± 0.2^{e}

Values are expressed as mean ± SEM (n=8). Scoring: 0 = absent, 1 = mild, 2 = moderate, 3 = severe. Different superscript letters indicate significant differences between groups ($p < 0.05$).

As a well-characterized experimental model, CCl_4-induced liver injury shares significant pathophysiological resemblance of human liver fibrosis and cirrhosis (Weiskirchen et al., 2019; Guo et al., 2025; Peng et al., 2025). The cascade of hepatotoxicity begins when CYP2E1 bioactivates CCl_4 to yield reactive trichloromethyl radicals which promote lipid peroxidation, protein carbonylation and DNA-damage (Sun et al., 2019; Algefare et al., 2024). The implementation of the hepatic damage was demonstrated in the present study with enhanced serum transaminases (ALT and AST), cholestatic markers (ALP, bilirubin) and synthetic function (decreased total protein), similar to previous studies (Soto et al., 2025; Fuertes-Agudo et al., 2023).

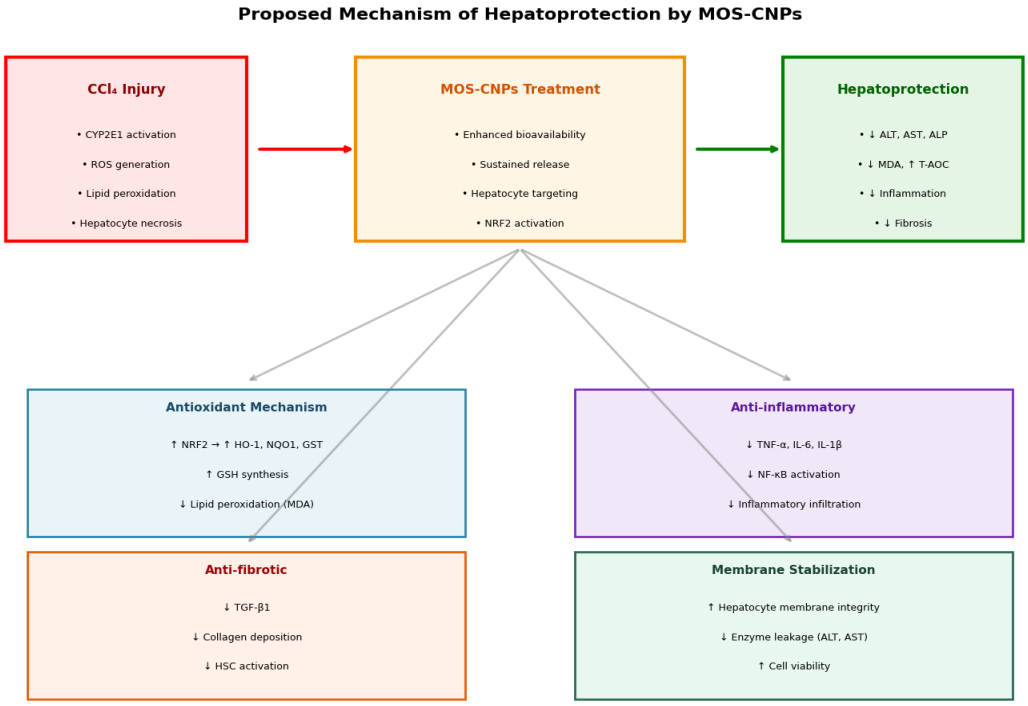

Figure 8. Proposed mechanism of hepatoprotection by MOS-CNPs against CCl_4-induced liver damage

The significant elevation of hepatic MDA (almost 4-fold) and depletion of T-AOC (75% reduction) in CCl_4-induced rats indicate severe oxidative destruction and breakdown of antioxidant system. These observations are consistent with some recent studies that chronic CCl_4 exposure generates mitochondrial injury, ER stress and the activation of pro-apoptotic pathways leading to hepatocyte necrosis and fibrogenesis (Guo et al., 2025; Peng et al., 2025). The dose-dependent amelioration of liver function markers by MOS-CNPs is an important therapeutic improvement. For the high-dose treatment (500 mg/kg), ALT, AST and ALP activities were nearly completely normalized to levels which were not statistically different from those of healthy controls. This is an outstanding activity exceeding those of typical *M. oleifera* preparations previously reported for hepatoprotective properties (Pari and Kumar, 2002; Aly et al., 2020). It is argued that enhanced hepatoprotection exhibited by MOS-CNPs can be attributed to several mechanisms: Improved bioavailability and cellular uptake: Chitosan nanoparticles protect entrapped phytochemicals from degradation in the stomach and first-pass metabolism and promote their absorption due to mucoadhesive in nature and transient opening of tight junctions (Rajabimashhadi et al., 2025; Jha and Mayanovic, 2023). The cationic surface charge of CNPs can facilitate electrostatic interaction with the negatively charged hepatocytes membrane, which further assists cellular uptake of bioactive compounds (Bonferoni et al., 2020). Sustained Release Effect: The sustained release profile of with initial burst release (35%) followed by slow and continuous drug dissolution for 48 hours, provides the maintenance of therapeutic dose over prolonged periods due to rapid clearance of free extract components (Rajabimashhadi et al., 2024). Presumably, this pharmacokinetic advantage accounts for the better efficacy that is seen

at equivalent or lower doses. Targeting the liver: Chitosan-based nanocarriers maintain natural affinity to hepatocytes through binding with asialoglycoprotein receptors and other membrane lectins, achieving targeted delivery to damaged organ (Bonferoni et al., 2020; Guo et al., 2025; Weiskirchen et al., 2019; ; Peng et al., 2025). The significant increase in total antioxidant capacity and the suppression of lipid peroxidation by MOS-CNPs imply strong activation of endogenous antioxidant systems. Moreover, the most relevant change is an increased expression of NRF2 (3.12-fold with the largest dose of MOS-CNPs) that shows induction of the master gene for antioxidant defenses (Cuadrado et al., 2019; Fuertes-Agudo et al., 2023). NRF2 activation leads to transcription induction of a variety of cytoprotective genes such as heme oxygenase-1 (HO-1), NAD(P)H quinone oxidoreductase 1 (NQO1), glutamate-cysteine ligase (GCL), and glutathione S-transferases (GSTs) that cumulatively increase cellular detoxification capability and antioxidant defense capacity (Cuadrado et al., 2019). The restored level of T-AOC may be due to increased de novo synthesis and recycling of glutathione, higher enzyme activity of antioxidant enzymes and scavenging of radicals by the phenolic compounds in the extract (Benzie & Strain, 1996; Mgheer et al., 2026). Bioactive phytochemicals of M. oleifera seeds, as especially isothiocyanates (derivatives of glucomoringin) and flavonoids (quercetin, kaempferol), are strong NRF2 activators that covalently modify cysteines from KEAP1 resulting in a conformational change leading authors to consider it loses its ability to sequester the nuclear protein NFR2 for exportation preventing translocation to nuclei (Singh et al., 2014; Pareek et al., 2023). Exposure of rats to NCFE exhibited liver cells with more pronounced nuclear NRF2 accumulation while little changes in this direction were noticed for FE alone. Nanoencapsulation seems to improve the delivery of these compounds within hepatocytes as compared to free extract, leading to clearer enhancement of NRF2 activation. The conventional dominance of MOS-CNPs to free MOS extract regarding all quantified factors implies that the role of drug carriers in herbal medicine is crucial. Even though the free extract at a dose of 250 mg/kg exerted significant protection, its nanoencapsulated equivalent (250 mg/kg of MOS-CNPs) caused significantly improved results, and that effect was further enhanced when doubling this dose (500 mg/kg), almost normalizing all parameters. However, this dose-sparing effect and improved efficacy are in accordance with the nanomedicine paradigm that particle deposition is accompanied by better pharmacokinetics for increased therapeutic indices (Gao et al., 2025). The findings indicate that MOS-CNPs may work at a pharmacologic dose under the therapeutic regimen of current preparations, reducing their doses required and costs, improving patient compliance, though also theoretically minimizing possible risk linked to phytochemical exposure. These results have important implications for drug intervention against hepato-protective therapy. Although the CCl_4 model does for sure not mimic all aspects of human liver disease, it is well suited to assess anti-oxidant and anti-fibrotic interventions (Weiskirchen et al., 2019). The efficacy of MOS-CNPs as revealed in this study indicate potentials for a wide range of liver diseases associated with oxidative stress such as NAFLD, alcoholic liver disease, drug induced hepatotoxicity and viral hepatitis. If the MOS-CNPs find a clinical application in future, some important areas that need to be considered for further research include: (1) pharmacokinetic studies comparing plasma and tissue levels of leading phytochemicals after intake of free extract versus MOS-CNPs; (2) examination of

additional signaling pathways such as NF-κB, AMPK, and/or PPAR-α which may contribute to hepatoprotection; (3) long-term safety and efficacy experiments in chronic liver disease models; and (4) scale-up and standardization of MOS-CNPs fabrication for potential clinical application (Gao et al., 2025).

Conclusion: This study shows that Moringa oleifera seeds ethanolic extract-loaded chitosan nanoparticles (MOS-CNPs) has hepatoprotective and antioxidants activity against CCl_4-induced hepatic derangement in male rats. The nano encapsulated formulation showed an enhanced efficacy than that of the free MOS extract, as observed by: Dose related restoration of liver function markers (ALT, AST, ALP, total bilirubin, total protein) with values reaching normal level in 500 mg/kg treated group. Strong antioxidant activity, as reflected by both the high T-AOC levels and low MDA contents, indicating inhibition of lipid peroxidation and maintenance of a balance between oxidation and antioxidation; Complete histopathological protection was observed overall for necrosis, inflammation, steatosis and fibrosis down to no pathology present in the high-dose group with near intact liver morphology; Strong activation of the NRF2 antioxidant pathway: MOS-CNPs 500 mg/kg upregulated the expression of NRF2 gene by 3.12-fold, indicating that it increases endogenous cytoprotective response. These results suggest MOS-CNPs as a potential nanomedicine for liver protection and further development for clinical applications in oxidative stress mediates liver damages. The improved bioavailability, sustain release effect and hepatocytes targeting efficiency suggest that the Chitosan NPs have made a remarkable progress in delivering Moringa oleifera therapeutic benefits towards hepatoprotection. Although we obtained promising findings, it is necessary to point out several limitations of this study. Our study was conducted exclusively in a rat model of CCl_4-induced liver injury. Therefore, caution is needed to generalize the results to human clinical conditions. We only assessed NRF2 gene expression. It would be beneficial in future studies to also assess the expression of downstream antioxidant target genes such as HO-1, NQO1, and GCLC, as this could provide deeper mechanistic insights into pathway activation. Future studies should investigate the pharmacokinetic parameters and tissue distribution of MOS-CNPs, and investigate long-term safety and toxicity studies of repeated administration of nanoparticles.

Author contributions

HAS and HHKA; Conceptualization and methodology, software and validation, formal analysis and investigation, resources, and data curation, HHKA, SHA, and HKA; writing-original draft preparation, writing-review, visualization, and funding acquisition.

Data availability statement

Data are available from the authors upon reasonable request.

Acknowledgements

The authors thanks all the staff of biochemistry and physiology department, veterinary medicine, Al-Qasim Green university for their supporting to complete this work.

Ethical considerations

The study was carried out with integrity, with no fabrication, falsification, plagiarism, or any scientific misconduct.

Funding

This research is supported by the Veterinary Medicine Collage, Al-Qasim Green University, Iraq.

Conflict of interest

The authors declare that there is no conflict of interest related to this research.

References

Abd-Elnaby, Y. A., ElSayed, I. E., AbdEldaim, M. A., Badr, E. A., Abdelhafez, M. M., & Elmadbouh, I. (2022). Anti-inflammatory and antioxidant effect of Moringa oleifera against bisphenol-A-induced hepatotoxicity. *Egyptian Liver Journal*, *12*, Article 57. https://doi.org/10.1186/s43066-022-00219-7

Algefare, A. I., Alfwuaires, M., Famurewa, A. C., Elsawy, H., & Sedky, A. (2024). Geraniol prevents CCl_4-induced hepatotoxicity via suppression of hepatic oxidative stress, pro-inflammation and apoptosis in rats. *Toxicology Reports*, *12*, 128–134. https://doi.org/10.1016/j.toxrep.2024.01.007

Aly, O., Abouelfadl, D. M., Shaker, O. G., Hegazy, G. A., Fayez, A. M., & Zaki, H. H. (2020). Hepatoprotective effect of Moringa oleifera extract on TNF-α and TGF-β expression in acetaminophen-induced liver fibrosis in rats. *Egyptian Journal of Medical Human Genetics*, *21*, Article 69. https://doi.org/10.1186/s43042-020-00106-z

Asrani, S. K., Devarbhavi, H., Eaton, J., & Kamath, P. S. (2019). Burden of liver diseases in the world. *Journal of Hepatology*, *70*(1), 151–171. https://doi.org/10.1016/j.jhep.2018.09.014

Benzie, I. F. F., & Strain, J. J. (1996). The ferric reducing ability of plasma (FRAP) as a measure of "antioxidant power": The FRAP assay. *Analytical Biochemistry*, *239*(1), 70–76. https://doi.org/10.1006/abio.1996.0292

Bonferoni, M. C., Gavini, E., Rassu, G., Maestri, M., & Giunchedi, P. (2020). Chitosan nanoparticles for therapy and theranostics of hepatocellular carcinoma (HCC) and liver-targeting. *Nanomaterials*, *10*(5), Article 870. https://doi.org/10.3390/nano10050870

Congyong, S., Wenjing, L., Yingkun, L., Wenwen, D., Adu-Frimpong, M., Huiyun, Z., Qilong, W., Jiangnan, Y., & Ximing, X. (2019). In vitro/in vivo hepatoprotective properties of 1-O-(4-hydroxymethylphenyl)-α-L-rhamnopyranoside from Moringa oleifera seeds against carbon tetrachloride-induced hepatic injury. *Food and Chemical Toxicology*, *131*, Article 110531. https://doi.org/10.1016/j.fct.2019.05.039

Cuadrado, A., Rojo, A. I., Wells, G., Hayes, J. D., Cousin, S. P., Rumsey, W. L., Attucks, O. C., Franklin, S., Levonen, A. L., Kensler, T. W., & Dinkova-Kostova, A. T. (2019). Therapeutic targeting of the NRF2 and KEAP1 partnership in chronic diseases. *Nature Reviews Drug Discovery*, *18*(4), 295–317. https://doi.org/10.1038/s41573-018-0008-x

Esterbauer, H., & Cheeseman, K. H. (1990). Determination of aldehydic lipid peroxidation products: Malonaldehyde and 4-hydroxynonenal. *Methods in Enzymology*, *186*, 407–421. https://doi.org/10.1016/0076-6879(90)86134-H

Fuertes-Agudo, M., Luque-Tévar, M., Cucarella, C., Martín-Sanz, P., & Casado, M. (2023). Advances in understanding the role of NRF2 in liver pathophysiology and its relationship with hepatic-specific cyclooxygenase-2 expression. *Antioxidants*, *12*(8), Article 1491. https://doi.org/10.3390/antiox12081491

Gao, F., Feng, X., & Li, X. (2025). Recent advances in polymeric nanoparticles for the treatment of hepatic diseases. *Frontiers in Pharmacology*, *16*, Article 1528752. https://doi.org/10.3389/fphar.2025.1528752

Guo, J., Lin, Y., Gong, X., Kuang, G., Hu, J., Du, H., Liu, H., Zhang, J., Zhang, L., Wan, J., & Wang, T. (2025). PROM2 exacerbates CCl_4-induced liver fibrosis via NLRP3 inflammasome activation and hepatocyte pyroptosis. *Cellular and Molecular Life Sciences*, *82*(1), Article 403. https://doi.org/10.1007/s00018-025-05920-5

Hammad, S., Ogris, C., Othman, A., Erdoesi, P., Schmidt-Heck, W., Biermayer, I., Helm, B., Gao, Y., Piorońska, W., Holland, C. H., D'Alessandro, L. A., de la Torre, C., Sticht, C., Al Aoua, S., Theis, F. J., Bantel, H., Ebert, M. P., Klingmüller, U., Hengstler, J. G., Dooley, S., & Mueller, N. S. (2023). Tolerance of repeated toxic injuries of murine livers is associated with steatosis and inflammation. *Cell Death & Disease*, *14*, Article 414. https://doi.org/10.1038/s41419-023-05855-4

Heidarpour, F., Mohammadabadi, M. R., Zaidul, I. S. M., Maherani, B., Saari, N., Hamid, A. A., Abas, F., Manap, M. Y. A., & Mozafari, M. R. (2011). Use of prebiotics in oral delivery of bioactive compounds: A nanotechnology perspective. *Pharmazie*, *66*(5), 319–324. https://doi.org/10.1691/ph.2011.0279

Jha, R., & Mayanovic, R. A. (2023). A review of the preparation, characterization, and applications of chitosan nanoparticles in nanomedicine. *Nanomaterials*, *13*(8), Article 1302. https://doi.org/10.3390/nano13081302

Livak, K. J., & Schmittgen, T. D. (2001). Analysis of relative gene expression data using real-time quantitative PCR and the 2^(-ΔΔCt) method. *Methods*, *25*(4), 402–408. https://doi.org/10.1006/meth.2001.1262

Mgheer, T. H., Al-Azawi, R. S. A., Mohi, W. Z., & Al-Shukri, H. H. K. (2026). Correlation of ACE (I/D) gene polymorphisms with type 2 diabetes mellitus and post-recovery from Covid-19 in Iraqi patients: A case-control investigation. *Agricultural Biotechnology Journal*, *18*(1), 281–300. https://doi.org/10.22103/jab.2025.26432.1812

Mohammadabadi, M. R., & Mozafari, M. R. (2018). Enhanced efficacy and bioavailability of thymoquinone using nanoliposomal dosage form. *Journal of Drug Delivery Science and Technology*, *47*, 445–453. https://doi.org/10.1016/j.jddst.2018.08.019

Mohammadabadi, M. R., & Mozafari, M. R. (2019). Development of nanoliposome-encapsulated thymoquinone: Evaluation of loading efficiency and particle characterization. *Journal of Biopharmaceuticals*, *11*(4), 39–46.

Mohammadabadi, M. R., El-Tamimy, M., Gianello, R., & Mozafari, M. R. (2009). Supramolecular assemblies of zwitterionic nanoliposome-polynucleotide complexes as gene transfer vectors: Nanolipoplex formulation and in vitro characterization. *Journal of Liposome Research*, *19*(2), 105–115. https://doi.org/10.1080/08982100802547326

Mohammed, A. J., Al-Awadi, H. K., & Al-Shukri, H. H. K. (2025). Synthesis and characterization of Aspartame and Neotame-encapsulated PLGA-TPGS nanoparticles and their modulatory effects on acetylcholinesterase gene expression in male rats. *Regulatory Mechanisms in Biosystems*, *16*(2), Article e25067. https://doi.org/10.15421/0225067

Mortazavi, S. M., Mohammadabadi, M. R., & Mozafari, M. R. (2005). Applications and in vivo behaviour of lipid vesicles. In M. R. Mozafari (Ed.), *Nanoliposomes: From fundamentals to recent developments* (pp. 67–76). Elsevier.

Omeodu, S. I., Eruotor, H. O., & Akpan, M. U. (2022). Effect of aqueous extract of Moringa oleifera leaves on some serum enzymes of Wistar rats with carbon tetrachloride-induced liver damage. *International Journal of Biochemistry Research & Review*, *31*(4), 17–23. https://doi.org/10.9734/ijbcrr/2022/v31i430315

Pareek, A., Pant, M., Gupta, M. M., Kashania, P., Ratan, Y., Jain, V., Pareek, A., & Chuturgoon, A. A. (2023). Moringa oleifera: An updated comprehensive review of its pharmacological activities, ethnomedicinal, phytopharmaceutical formulation, clinical, phytochemical, and toxicological aspects. *International Journal of Molecular Sciences*, *24*(3), Article 2098. https://doi.org/10.3390/ijms24032098

Pari, L., & Kumar, N. A. (2002). Hepatoprotective activity of Moringa oleifera on antitubercular drug-induced liver damage in rats. *Journal of Medicinal Food*, *5*(3), 171–177. https://doi.org/10.1089/10966200260398206

Peng, M., Fang, F., & Wang, B. (2025). Nanoparticle technologies for liver targeting and their applications in liver diseases. *Frontiers in Pharmacology*, *16*, Article 1661872. https://doi.org/10.3389/fphar.2025.1661872

Rajabimashhadi, Z., Masi, A., Bagheri, S., Mele, C., Colangelo, G., Paladini, F., & Pollini, M. (2025). Development and characterization of chitosan microparticles via ionic gelation for drug delivery. *Polymers*, *17*(19), Article 2603. https://doi.org/10.3390/polym17192603

Singh, D., Arya, P. V., Aggarwal, V. P., & Gupta, R. S. (2014). Evaluation of antioxidant and hepatoprotective activities of Moringa oleifera Lam. leaves in carbon tetrachloride-intoxicated rats. *Antioxidants*, *3*(3), 569–591. https://doi.org/10.3390/antiox3030569

Soto, J. A., Gómez, A. C., Vásquez, M., Barreto, A. N., Molina, K. S., & Zúñiga-González, C. A. (2025). Biological properties of Moringa oleifera: A systematic review of the last decade. *F1000Research*, *13*, Article 1390. https://doi.org/10.12688/f1000research.157194.2

Tao, L., Gu, F., Liu, Y., Yang, M., Wu, X.-Z., Sheng, J., & Tian, Y. (2022). Preparation of antioxidant peptides from Moringa oleifera leaves and their protection against oxidative damage in HepG2 cells. *Frontiers in Nutrition*, *9*, Article 1062671. https://doi.org/10.3389/fnut.2022.1062671

Weiskirchen, R., Weiskirchen, S., & Tacke, F. (2019). Organ and tissue fibrosis: Molecular signals, cellular mechanisms and translational implications. *Molecular Aspects of Medicine*, *65*, 2–15. https://doi.org/10.1016/j.mam.2018.06.003

Zarrabi, A., Alipoor Amro Abadi, M., Khorasani, S., Mohammadabadi, M., Jamshidi, A., Torkaman, S., Taghavi, E., Mozafari, M. R., & Rasti, B. (2020). Nanoliposomes and tocosomes as multifunctional nanocarriers for the encapsulation of nutraceutical and dietary molecules. *Molecules*, *25*(3), Article 638. https://doi.org/10.3390/molecules25030638

مجله بیوتکنولوژی کشاورزی
شاپا چاپی: ۶۷۰۵-۲۲۲۸ شاپا الکترونیکی: ۶۵۰۰-۲۲۲۸

اثر محافظتی کبدی عصاره بذر *Moringa oleifera* بارگذاری‌شده در نانوذرات کیتوزان (MOS-CNPs)از طریق القای بیان ژن NRF2 در برابر آسیب کبدی القاشده با CCl_4 در رت‌های نر

حیدر علی صاحب

دانشکده دامپزشکی، دانشگاه القاسم سبز، ۵۱۰۱۳ بابل، عراق. ایمیل: hayderali@vet.uoqasim.edu.iq

حسن کاطع العوادی

دانشکده دامپزشکی، دانشگاه القاسم سبز، ۵۱۰۱۳ بابل، عراق. ایمیل: Dr.hassan@uoqasim.edu.iq

حمزه هاشم الشکری

نویسنده مسئول. دانشکده دامپزشکی، دانشگاه القاسم سبز، ۵۱۰۱۳ بابل، عراق. ایمیل: hamza.hashim@vet.uoqasim.edu.iq

تاریخ دریافت: ۱۴۰۴/۱۰/۰۳ تاریخ دریافت فایل اصلاح شده نهایی: ۱۴۰۴/۱۱/۲۸ تاریخ پذیرش: ۱۴۰۴/۱۱/۲۹

چکیده

هدف: بیماری‌های کبدی یکی از مشکلات عمده سلامت در سراسر جهان هستند و استرس اکسیداتیو در پاتوژنز آسیب‌های کبدی ناشی از مواد شیمیایی نقش دارد. بذرهای *Moringa oleifera* (مورینگا اولیفرا) دارای فعالیت‌های آنتی‌اکسیدانی و محافظت‌کننده کبدی قوی هستند، اما فراهمی زیستی پایین، کارایی آن‌ها را محدود می‌کند. نانوذرات کیتوزان (CNPs) به‌عنوان سامانه‌های انتقالی چندمنظوره برای ترکیبات زیست‌فعال شناخته می‌شوند که موجب بهبود ویژگی‌های فارماکوکینتیکی می‌گردند. هدف این مطالعه بررسی اثرات محافظت‌کننده کبدی و آنتی‌اکسیدانی عصاره اتانولی بذر مورینگا (MOSEE) بارگذاری‌شده در نانوذرات کیتوزان (MOS-CNPs) در برابر آسیب کبدی القاشده با تتراکلرید کربن (CCl_4) در رت‌های نر بود.

مواد و روش‌ها: چهل رت نر به‌طور تصادفی به پنج گروه (n=8) تقسیم شدند: گروه کنترل (سالین نرمال/روغن زیتون)، گروه دریافت‌کننده CCl_4 (کنترل منفی)، گروه CCl_4 + عصارهMOS ، گروه CCl_4 + MOS-CNPs با دوز پایین، و گروه CCl_4 + MOS-CNPs با دوز بالا. مدت آزمایش ۸ هفته بود. شاخص‌های بیوشیمیایی شامل آلانین آمینوترانسفراز (ALT)، آسپارتات آمینوترانسفراز(AST) ، آلکالین فسفاتاز (ALP)، پروتئین تام (TP) و بیلی‌روبین تام (TB) اندازه‌گیری شد. وضعیت آنتی‌اکسیدانی از طریق ظرفیت آنتی‌اکسیدانی کل (T-AOC) و سطح مالون‌دی‌آلدئید (MDA) ارزیابی گردید. همچنین بافت کبد از نظر آسیب‌شناسی بافتی بررسی و بیان ژن NRF2 با روش qRT-PCR اندازه‌گیری شد.

نتایج: تیمار با CCl_4 موجب افزایش معنی‌دار (217.95±9.87 U/L) ALT، (200.89±12.45 U/L) AST، ALP (320.91±15.67 U/L) و بیلی‌روبین تام (2.76±0.24 mg/dL) و کاهش پروتئین تام (4.15±0.28 g/dL) نسبت به گروه

کنترل شد ($p<0.001$). درمان با MOS-CNPs به‌صورت وابسته به دوز، این تغییرات را معکوس کرد و بهترین نتایج در گروه دوز بالا مشاهده شد: ALT (77.96±5.12 U/L)، AST (79.69±6.23 U/L)، ALP (155.98±10.45 U/L)، TB (0.99 ± 0.08 mg/dL)، و TP (6.99 ± 0.32 g/dL). تجویز MOS-CNPs با دوز ۵۰۰ mg/kg باعث افزایش معنی‌دار T-AOC (4.46±0.21 mmol/L) و کاهش MDA (3.06±0.25 µmol/L) در مقایسه با گروه CCl_4 شد ($p<0.001$). بیان ژن NRF2در گروه‌های دریافت‌کننده MOS-CNPs به‌طور چشمگیری افزایش یافت. یافته‌های بافت‌شناسی نیز کاهش نکروز سلول‌های کبدی، نفوذ سلول‌های التهابی و دژنراسیون چرب را تأیید کردند.

نتیجه‌گیری: نانوذرات کیتوزان حاوی عصاره بذر مورینگا (MOS-CNPs) در مقایسه با عصاره آزاد، به دلیل فراهمی زیستی بهتر و الگوی آزادسازی کنترل‌شده، اثر محافظت‌کننده کبدی و آنتی‌اکسیدانی قوی‌تری نشان دادند. دوز بالای ۵۰۰ mg/kg بیشترین محافظت را در برابر آسیب کبدی ناشی از CCl_4 از طریق تنظیم استرس اکسیداتیو و فعال‌سازی مسیر سیگنال‌دهی آنتی‌اکسیدانی NRF2فراهم کرد.

کلمات کلیدی: آنزیم‌های کبدی، استرس اکسیداتیو، محافظت کبدی، نانودارو، نانوذرات کیتوزان

نوع مقاله: پژوهشی

استناد: حیدر علی صاحب، حسن کاظم العوادی، حمزه هاشم ال‌شکری (۱۴۰۵) اثر محافظتی کبدی عصاره بذر Moringa oleifera بارگذاری‌شده در نانوذرات کیتوزان (MOS-CNPs) از طریق القای بیان ژن NRF2 در برابر آسیب کبدی القاشده با CCl_4 در رت‌های نر. *مجله بیوتکنولوژی کشاورزی*، ۱۸(۲)، ۴۶۷-۴۸۸.

Publisher: Shahid Bahonar University of Kerman & Iranian Biotechnology Society.